

Attenuation of Second Sound in Helium II between Rotating Cylinders*

PHILIP J. BENDT†

Los Alamos Scientific Laboratory, University of California, Los Alamos, New Mexico

(Received 10 August 1966)

In an annular resonant cavity, we have shown that the attenuation of second sound is the same for solid-body rotation, rotation of the outside cylinder only, and rotation of the inside cylinder only, if plotted against $|\text{curl } \mathbf{v}_s|$, where the superfluid velocity \mathbf{v}_s is calculated by classical hydrodynamics. Additional attenuation due to secondary flow was observed when the inside cylinder only rotated faster than 0.4 rad/sec. In solid-body rotation, we find that the attenuation plotted as a function of angular velocity deviates from linearity by not more than 1%, out to 6 rad/sec. We measured the perpendicular mutual-friction coefficient B at 50-mdeg intervals between 1.2 and 2.08°K, with an uncertainty of $\pm 2\%$ in the smoothed values; our values of B are 4 to 8% higher than previous measurements by Hall and Vinen. We also measured the velocity of second sound to $\pm 1\%$.

I. INTRODUCTION

RECENTLY Hall and Vinen¹ showed that the attenuation of second sound in rotating helium II is due to mutual friction between the excitations which comprise the normal fluid and vortex lines in the superfluid. In the Feynman-Onsager model, the density of vortex lines is given by $(m/h)|\text{curl } \mathbf{v}_s|$.² We have tested the hypothesis that the attenuation is proportional to the $|\text{curl } \mathbf{v}_s|$ in an annular second-sound resonant cavity, whose cylindrical walls could be rotated independently, by comparing the attenuation for three different forms of Couette flow.

The perpendicular mutual friction coefficient B is used to check detailed theories of the scattering of rotons by vortex lines.¹ To provide better data for this purpose, we have measured the temperature dependence of B with improved precision. Measurements were made using a cavity with an order of magnitude larger Q than used by Hall and Vinen. The increased sensitivity which results from a high Q cavity made possible a careful investigation of the linearity of the attenuation with vortex line density.

II. APPARATUS

A cross-section view of the annular second-sound resonant cavity is shown in Fig. 1. The cylindrical walls were anodized aluminum, and could be rotated independently by concentric shafts which passed through O-ring seals at the top of the cryostat. The cylinders were rotated by a Vickers hydraulic variable speed transducer, driven by a synchronous motor. The

transducer changed the angular velocity of the cylinder it was driving at 0.07 rad/sec², and the maximum angular velocity was 6 rad/sec. The cylinders were rotated in four ways: (1) solid-body rotation; (2) the inside cylinder only was rotated; (3) the outside cylinder only was rotated; (4) the outside cylinder was rotated by the Vickers transducer, and the inside cylinder was rotated $\frac{2}{3}$ as fast, in the same direction, by a gear train connecting the two drive shafts. The radii of the cylinders were machined so $R_2^2/R_1^2 = 1.500$, so this type of rotation produced potential flow.

The cylinders were placed near the bottom of a glass cryostat which held 5 liters of liquid helium. Temperatures down to 1.2°K were achieved by pumping on the

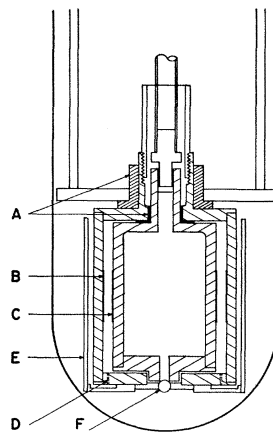


FIG. 1. Cross-section view of the annular second-sound resonant cavity. The two bearings A are Kel-F. The resonant space is between the Aquadag second-sound heater B and the Aquadag detector C. dc heating in the cavity is removed by counterflow of helium II through 180.055-in. holes D, laid out in a circle on the bottom plate, at the temperature node for the half-wavelength radial mode. These holes connect with helium which rotates with the outside cylinder, since the aluminum shield E is attached to the bottom of the cavity. For the measurements with solid-body rotation, a Kel-F sleeve at the bottom of the cylinders, similar to A, kept the two cylinders concentric. For other forms of rotation, a $\frac{1}{4}$ -in. steel ball F formed the bottom bearing. The inside dimensions of the resonant cavity at room temperature were: length, 3.193 in.; i.d., 2.143 in.; o.d., 2.624 in.

* Work performed under the auspices of the U. S. Atomic Energy Commission.

† Present address: Physics Department, University of Oregon, Eugene, Oregon.

¹ H. E. Hall and W. F. Vinen, Proc. Roy. Soc. (London) **A238**, 204 (1956); **A238**, 215 (1956); H. E. Hall, Advan. Phys. **9**, 89 (1960); E. L. Andronikashvili and Yu. G. Mamaladze, Rev. Mod. Phys. **38**, 567 (1966).

² R. P. Feynman, in *Progress in Low Temperature Physics*, edited by C. J. Gorter (North-Holland Publishing Company, Amsterdam, 1955), Vol. I, p. 17; m is the mass of a helium-4 atom, h is Planck's constant, and \mathbf{v}_s is the superfluid velocity.

helium with a Kinney KDH-130 vacuum pump. The helium bath temperature was maintained constant within a millidegree with a Sommers electronic temperature regulator.³

The second-sound heater and detector were 1-in.-wide Aquadag coatings painted completely around each cylinder (Fig. 1). A $\frac{1}{16}$ -in. conducting strip of DuPont electronic grade silver preparation was painted on the top and bottom edges of each Aquadag band. The resistance R of the Aquadag detector, and also $(1/R)(dR/dT)$, are shown in Fig. 2 as a function of temperature T . Mercury troughs were used for electrical connections with the rotating parts. A Hewlett Packard (HP) 651A test oscillator was used to generate the second sound; the oscillator was modified so that one turn of a helipot changed the frequency by 1 cps. The signal from the second-sound detector was amplified by a Tektronix 122 preamplifier, and passed through a filter to a HP 400E ac voltmeter, which was used as an amplifier and ac to dc converter. Two chart recorders were used to record the voltage amplitude of the oscillator and of the second-sound signal. The frequency of the oscillator was measured to one part in 10^6 with a HP 5243L frequency counter.

III. PRECISION OF THE CAVITY

The width D of the annulus between the Aquadag coatings at 1.5°K was 0.608 ± 0.002 cm, approximately equal to $\frac{1}{3}$ the mean radius of the cylindrical walls. The fundamental radial mode waveform was the superposition of two Bessel functions: $J_0(2\pi r/\lambda)$ and $\xi Y_0(2\pi r/\lambda)$, where r is the radial distance from the axis, λ is the second-sound wavelength, and ξ is a constant, approximately equal to -1.30 . To the accuracy with which the width of the annulus is known, $\lambda = 2D$, the same as for a plane wave.

The surface roughness of the anodized aluminum cylinders and Aquadag coatings was measured with a Bendix Proficorder, and was about $30 \mu\text{in.}$ The thickness of the Aquadag coatings was about $100 \mu\text{in.}$, and the thickness of the DuPont conducting strips was about $300 \mu\text{in.}$

We define the Q of the cavity as $f/\Delta f$, where f is the resonant frequency, and Δf is the *full width* of the resonance at $\frac{1}{2}\sqrt{2}$ of the maximum amplitude, as measured with a frequency counter.⁴ The Q of the cavity in its fundamental radial mode varied somewhat from run to run, but average values as a function of temperature are given in Fig. 2. The Q is dependent to a large extent on the geometrical perfection of the cavity. We may write $Q^{-1} = Q_g^{-1} + Q_h^{-1}$, where Q_g is the geometrical Q which would result if there were no dissipation of second-sound energy, and Q_h is the dissipation Q which

³ H. S. Sommers, Rev. Sci. Instr. **25**, 793 (1954).

⁴ In Refs. (1) and (6), Δf in the expression for Q is the *halfwidth* of the resonance. For this reason, some of their equations differ from ours by a factor of 2, and the numerical values of Q they give are twice as large as we give for the same resonance widths.

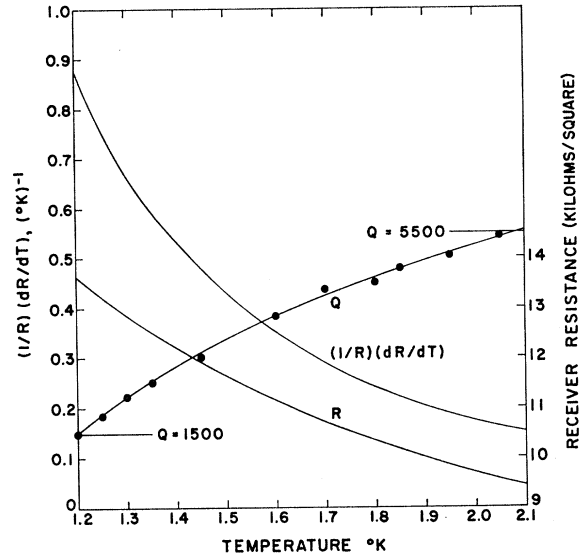


Fig. 2. Graphs of the Q of the annular second-sound resonant cavity in its fundamental radial mode (Q equals 10^4 times the scale on the left), of the resistance R of the Aquadag second-sound detector (R in ohms/square equals 10^3 times the scale on the right), and of $(1/R)(dR/dT)$. The resistance of the second-sound heater is $\frac{1}{4}$ that of the detector. Experimental points are for Q .

would result if the cavity were geometrically perfect. The temperature dependence of Q is due entirely to Q_h .⁵ The largest Q observed (5500) sets a lower limit on Q_g . An estimate of the variation, equal to $\pm d$, in the width of the annulus (over distances of the order of a wavelength) is given by $d = D/2Q_g$. Setting $Q_g = 5500$ gives an upper limit for d of $22 \mu\text{in.}$

A problem in the construction of the cavity was to minimize the variation in the *average* width of the annulus when the cylindrical walls were rotated relative to each other. The difficulty was that the frequency of the sharply peaked cavity resonance would vary with a periodicity determined by the relative angular velocity of the cylinders. Substitution of the steel ball F (Fig. 1) in place of the original Kel-F bearing at the bottom of the cavity considerably improved the stability of the resonant frequency. The variation in average width with rotation was reduced to $20 \mu\text{in.}$

IV. THEORY

Following the analysis of Hall and Vinen,¹ the mutual friction force per unit volume acting on the normal fluid is given by

$$\mathbf{F}_{sn} = \frac{\rho_s \rho_n}{\rho} \frac{|\text{curl} \mathbf{v}_s|}{2} [B(\mathbf{v}_s' - \mathbf{v}_n') + B'(\mathbf{v}_s' - \mathbf{v}_n') \times \hat{\Omega}], \quad (1)$$

⁵ The question arises whether, if $Q_g \gg Q_h$, the Q of the cavity can be used to determine the liquid-helium attenuation coefficient α for the second-sound amplitude A in the relation $A(x) = A_0 \exp(-\alpha x)$. The cavity walls are not perfectly reflecting, and losses at the walls predominate over losses in the liquid. The coefficient α has been measured by a different method by W. B. Hanson and J. R. Pellam, Phys. Rev. **95**, 321 (1954).

where \mathbf{v}_s is the average superfluid velocity neglecting vortex lines; \mathbf{v}_s' and \mathbf{v}_n' refer to the second-sound wave, and are parallel to the second-sound propagation; B and B' are mutual friction coefficients, and $\hat{\Omega}$ is an axial unit vector in the direction of rotation. Our experiment observes the attenuation due to the first term; the second term is not dissipative, since it is perpendicular to $(\mathbf{v}_s' - \mathbf{v}_n')$.

Let α be the attenuation coefficient for the second-sound amplitude in the expression $A(x) = A_0 \exp(-\alpha x)$. In rotating helium $\alpha = \alpha_0 + \alpha_r$, where α_0 applies to stationary helium, and α_r is due to \mathbf{F}_{sn} . If a damping term due to \mathbf{F}_{sn} is included in the wave equation for second-sound, then

$$\alpha_r = B |\text{curl } \mathbf{v}_s| / 4u_2, \quad (2)$$

where u_2 is the velocity of second sound.

The Q of a resonant cavity in its fundamental mode is related to α by $\alpha = \pi / \lambda Q$, and is related to α_r by

$$\alpha_r = \frac{\pi}{\lambda Q_0} \left[\frac{A_0}{A(\Omega)} - 1 \right], \quad (3)$$

where Q_0 refers to the cavity at rest, and we have substituted the ratio of second-sound amplitudes $A_0/A(\Omega)$ for the equivalent ratio $Q_0/Q(\Omega)$. We refer to $[A_0/A(\Omega) - 1]$ as the "attenuation." Equating Eqs. (2) and (3) gives

$$B = \frac{4\pi f}{Q_0 |\text{curl } \mathbf{v}_s|} \left[\frac{A_0}{A(\Omega)} - 1 \right], \quad (4)$$

where $|\text{curl } \mathbf{v}_s|$ is calculated from the angular velocities of the cylindrical walls, and the other quantities are measured. A plot of the attenuation versus $|\text{curl } \mathbf{v}_s|$ should give a straight line with a slope equal to $BQ_0/4\pi f$, according to this analysis.

Primary flow of a viscous fluid between concentric rotating cylinders is restricted to the form

$$\mathbf{v} = \hat{\Omega}(Ar + B/r), \quad (5)$$

where r is the radius and A and B are constants. Our experiments show that in steady state, the superfluid flow also satisfies Eq. (5). The $|\text{curl } \mathbf{v}| = 2A$, and has the following values for the forms of Couette flow we used: solid-body rotation, $2\Omega_1$; rotation of the inside cylinder only, $4\Omega_1$; rotation of the outside cylinder only, $6\Omega_2$; potential flow ($\Omega_1 R_1^2 = \Omega_2 R_2^2$), zero (angular velocity Ω_1 and radius R_1 refer to the inside cylinder, and Ω_2 and R_2 to the outside cylinder).

The flow during solid-body rotation, and rotation of the outside cylinder only, is stable primary flow at all angular velocities. The flow during rotation of the inside cylinder only was stable out to $\Omega_1 = 0.4$ rad/sec (at 1.400°K); at higher angular velocities additional attenuation of second sound was observed. This was due to the vorticity in secondary flow. Secondary flow

is caused by centrifugal force on the fluid adjacent to the inside cylinder. The secondary flow of a classical fluid would be in the form of toroids (Taylor cells), which circle the inside cylinder.

In primary *potential* flow, there should be no vortex lines in the superfluid, and no attenuation of second sound. We observed attenuation due to secondary flow when Ω_1 was larger than a critical angular velocity, which depended on the temperature.

V. SOLID-BODY ROTATION

We wish to describe three types of measurements which were made preliminary to our measurements of B as a function of temperature. The first of these is shown in Fig. 3, where the second-sound signal from our annular resonant cavity is plotted against ac power input to the second-sound heater, at temperatures between 2.00 and 2.10°K. Similar measurements at lower temperatures always yielded a straight line, similar to the measurements at 2.00°K. These data were taken to establish that the power density at which we made attenuation measurements was below the level at which the second-sound standing wave was saturated. Above 2.00°K, the power level was restricted to 0.2 mW/cm².

In Fig. 4, the second-sound signal is plotted as divisions on the chart recorder against heater power in mW/cm², for the cylinders at rest, and for three angular velocities of solid-body rotation. The attenuation measurements described below were made at a constant heater power, which would be along a line parallel to the ordinate in Fig. 4. The fact that Fig. 4 displays straight

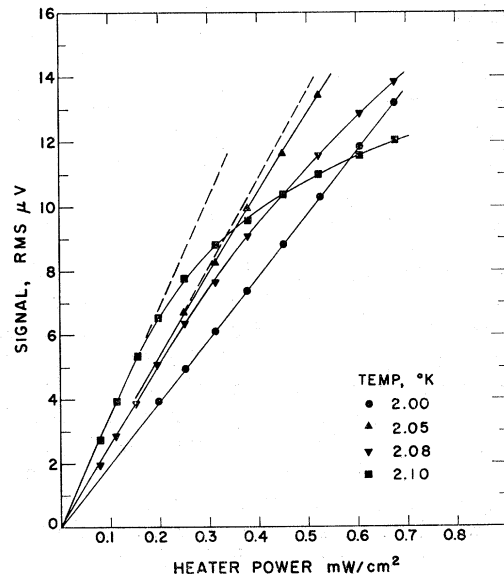


FIG. 3. Amplitude of the second-sound signal when the detector was biased with 0.02 mA dc per cm of circumference, plotted against ac power input to the second-sound heater. The curves taken at $T > 2.00^\circ\text{K}$ show saturation of the second-sound standing wave in the resonant cavity.

lines which pass through the origin is additional assurance that the attenuation we measured was independent of heater power.

Hall and Vinen¹ assumed that the attenuation of second sound is linearly dependent on the density of vortex lines. This implies that the scattering of excitations by one vortex line is not affected by the presence of other vortex lines, and is justified by the fact that the distance between vortex lines is very much larger than the roton mean free path, at $T \geq 1.2^\circ\text{K}$. As they measured the attenuation at only three angular velocities, this assumption was not thoroughly tested in their experiments. We have carefully tested this assumption at 1.40°K , by making attenuation measurements at 18 angular velocities between zero and 6 rad/sec, with an accuracy on each point of $\pm 2\%$. We can report that the deviation of the attenuation from linearity, when plotted against angular velocity, is not greater than 1% at this temperature. At other temperatures between 1.2 and 2.08°K , six attenuation measurements were usually made between zero and 4 rad/sec, and no deviation from linearity was observed at any temperature.

A portion of the attenuation curve at 1.40°K is shown in Fig. 5. To make steady-state attenuation measurements, such as are shown in Fig. 5, it is necessary to wait from 6 to 12 min after the cylinders are accelerated to a new angular velocity, for the transient attenuation to decay.

Our principal result with solid-body rotation is the measurement of the mutual friction coefficient B as a

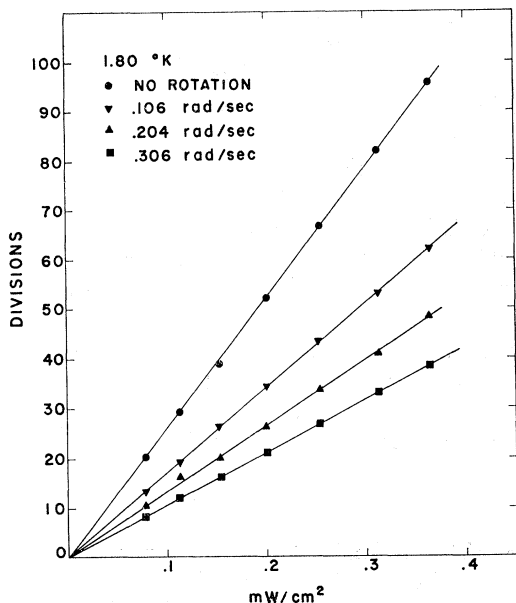


FIG. 4. Amplitude of the second-sound signal, plotted as divisions on the chart recorder, against ac power input to the second-sound heater. The different straight lines refer to the cylinders at rest, and with constant solid-body rotation at the specified angular velocities. Attenuation measurements result from plotting the intersections of these lines with a line for constant mW/cm^2 (parallel to the ordinate).

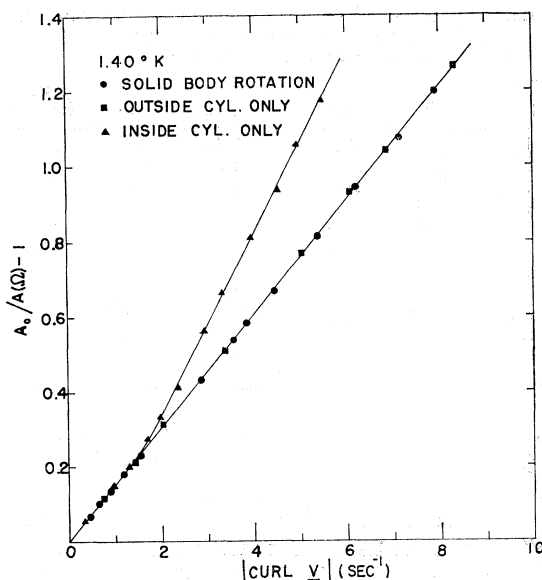


FIG. 5. The attenuation of second sound at 1.40°K , plotted against $|\text{curl } \mathbf{v}|$ for three forms of Couette flow. The figure illustrates three things: first, the linearity of the attenuation as the vortex line density increases; second, the fact that the $\text{curl } \mathbf{v}$ can be calculated by classical hydrodynamics from the angular velocities of the rotating cylinders; and third, the additional attenuation resulting from secondary flow when the inside cylinder only is rotated faster than 0.4 rad/sec .

function of temperature, shown in Fig. 6. Smoothed values of B are listed in Table I. Each point in Fig. 6 is calculated from the slope of a straight-line attenuation

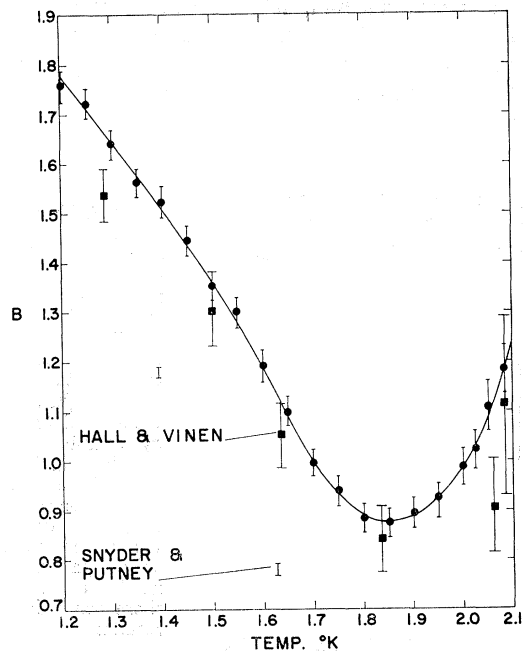


FIG. 6. The perpendicular mutual-friction coefficient B as a function of temperature. For the significance of B , see Eqs. (1), (2), and (4). The points "Hall and Vinen" are from Ref. 1, and "Snyder and Putney" are from Ref. 6.

TABLE I. Smoothed values of the perpendicular mutual-friction coefficient B and of the velocity of second sound u_2 .

Temp. (°K)	B	u_2 (m/sec)	Temp. (°K)	B	u_2 (m/sec)
1.20	1.78	18.6	1.70	1.00	20.3
1.25	1.72	18.8	1.75	0.94	20.2
1.30	1.65	19.1	1.80	0.89	19.9
1.35	1.58	19.3	1.85	0.88	19.4
1.40	1.51	19.6	1.90	0.89	18.8
1.45	1.44	19.8	1.95	0.93	17.9
1.50	1.36	20.0	2.000	0.99	16.6
1.55	1.29	20.2	2.025	1.03	15.8
1.60	1.19	20.3	2.050	1.09	14.9
1.65	1.09	20.4	2.075	1.16	13.7
			2.100	1.24	12.3

curve, such as Fig. 5. Since the slope is proportional to the Q of the cavity, the slopes we measured were 6 to 20 times larger than those measured by Hall and Vinen.¹ We therefore claim higher precision on each point; $\pm 2\%$ from 1.2 to 1.9°K, decreasing to $\pm 4\%$ at 2.08°K. The smoothed values in Table I should be accurate to $\pm 2\%$.

Our measurements at closely spaced temperatures have clarified the temperature dependence of B . Our measurements are 4 to 8% larger than the earlier measurements by Hall and Vinen, if we neglect their point at 2.06°K. The two measurements in Fig. 6 by Snyder and Putney⁶ were made in a rectangular cavity having a Q about equal to that of Hall and Vinen. We suspect their measurements are low because of the difficulty in measuring Q_0 with a phase-sensitive detector. Table I also gives smoothed values of the velocity of second sound, determined from the resonant frequency of our high- Q cavity. The values should be accurate to $\pm 1\%$ and are in good agreement with recent measurements by Mercereau, Notarys, and Pellam.⁷

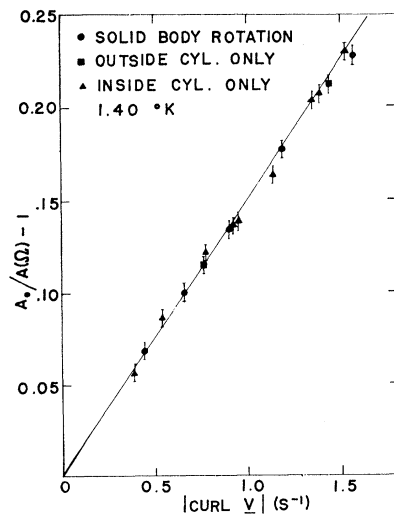


FIG. 7. The portion of Fig. 5 near the origin, plotted with expanded scales. Six additional points for the "inside cylinder only" are shown, which were taken on two additional runs. The straight line has the slope determined by solid-body rotation in Fig. 5. This figure shows that the attenuation measurements for rotation of the inside cylinder only (in primary flow) agree with those for solid-body rotation.

VI. OTHER FORMS OF ROTATION

The second-sound attenuation for other forms of primary Couette flow should depend only on the $|\text{curl } \mathbf{v}_s|$. We have shown at 1.40°K that the vorticity of superfluid between concentric rotating cylinders is the same as for a classical fluid. This follows from Figs. 5 and 7, where the attenuation for three types of rotation is plotted against the $|\text{curl } \mathbf{v}|$ calculated from the angular velocity of the cylinders by classical hydrodynamics (refer to Sec. IV). Good agreement was obtained between solid-body rotation and rotation of the outside cylinder only; rotation of the inside cylinder only also agrees until secondary flow occurs, when $|\text{curl } \mathbf{v}_s| > 1.6 \text{ sec}^{-1}$.

Our results on potential flow, for which $\Omega_1 R_1^2 = \Omega_2 R_2^2$, have been published elsewhere,⁸ and will be summarized only. Transient attenuation was observed each time the angular velocity of the cylinders was increased, but no steady-state attenuation was observed until the onset of secondary flow. This supports the hypothesis that, since $\text{curl } \mathbf{v}$ is zero in potential flow, there would be no vortex lines in the superfluid to attenuate the second sound. The onset of secondary flow was temperature-dependent (because the superfluid- and normal-fluid densities change), and varied from $\Omega_1 = 0.30 \text{ rad/sec}$ at 1.247°K to 0.63 rad/sec at 2.001°K. Assigning an eddy viscosity to the superfluid of $30 \mu\text{P}$, the onset of secondary flow at six temperatures was correlated by means of a superfluid Reynolds number N_s , based on the radius and surface velocity of the inside cylinder; the average value of N_s was 11 500.

The absence of vortex lines in the primary flow makes second sound a sensitive tool to locate hydrodynamic transitions in the secondary flow. Four transitions were observed in the flow at 1.80°K, between zero and 4.48 rad/sec. The distinctive break at 4.48 rad/sec was observed at 2.95 rad/sec at 1.950°K and at 2.38 rad/sec at 2.001°K. These breaks give a reasonably consistent Reynolds number N_n based on the normal-fluid viscosity and density; the average value of N_n was 97 100. The vorticity in secondary flow could be measured from the attenuation curves. If the liquid helium was stirred after cooling through the lambda transition, the breaks in the attenuation curves were smoothed out, and barely discernable.

ACKNOWLEDGMENTS

We wish to thank Clarence Harmer and Donald Clinton of the Los Alamos Scientific Laboratory Shops Department for the precision machining of the cylinders and bearings of the annular resonant cavity.

⁶ H. A. Snyder and Z. Putney, *Phys. Rev.* **150**, 110 (1966).

⁷ J. Mercereau, H. Notarys, and J. R. Pellam, in *Proceedings of*

the Seventh International Conference on Low Temperature Physics (University of Toronto Press, Toronto, Canada, 1961), Paper 23-7.

⁸ P. J. Bendt, *Phys. Rev. Letters* **17**, 680 (1966).